Title

IDA STUDY OF THE UNBURNED GAS MOTION INDUCED BY NONSTEADY FLAME PROPAGATION IN A CONSTANT VOLUME DUCT

Authors

Dunn-Rankin, D.
Sawyer, R.F.

Publication Date

1985-02-01

Lawrence Berkeley Laboratory

UNIVERSITY OF CALIFORNIA

APPLIED SCIENCE DIVISION

To be presented at the Joint Technical Meeting,
Central States Section/Western States Section/
The Combustion Institute, San Antonio, TX,
April 22-23, 1985

LDA STUDY OF THE UNBURNED GAS MOTION INDUCED BY NONSTEADY FLAME PROPAGATION IN A CONSTANT VOLUME DUCT

D. Dunn-Rankin and R.F. Sawyer

February 1985

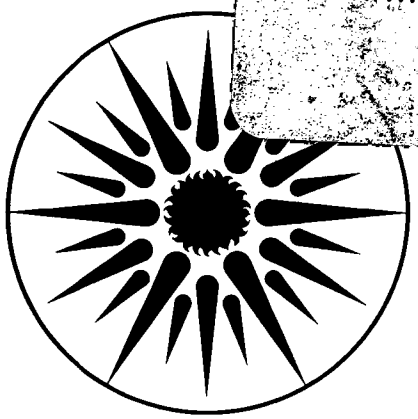

APPLIED SCIENCE DIVISION

Prepared for the U.S. Department of Energy under Contract DE-AC03-76SF00098

DISCLAIMER

LDA STUDY OF THE UNBURNED GAS MOTION INDUCED BY NONSTEADY FLAME PROPAGATION IN A CONSTANT VOLUME DUCT

D. Dunn-Rankin and R.F Sawyer

Lawrence Berkeley Laboratory, Applied Science Division
University of California, Department of Mechanical Engineering
Berkeley, CA 94720

This work was supported by the Assistant Secretary for Conservation and Renewable Energy, Office of Transportation Programs, Division of Transportation Energy of the U.S. Department of Energy under contract number DE-AC03-76SF00098.

ABSTRACT

The objective of this work is to improve the understanding of fluid motion generated by premixed combustion in a constant volume enclosure. Velocity measurements, using laser Doppler anemometry, provide a mapping of the velocity field generated during flame propagation in a closed duct (38 mm x 38 mm x 155 mm). The combustible gas is a stoichiometric mixture of methane and air.

Both the flame shape and the unburned gas motion affect the burned gas flow field. The unburned gas velocity field, however, is insensitive to flame shape changes, and is nearly one-dimensional except very near the flame front. A one-dimensional model of the unburned gas accurately predicts the relationship between the velocity, the flame area, and the chamber pressure.

INTRODUCTION

Combustion generated flow in a system with a well defined flame front arises naturally as consequence of mass conservation across the flame:

$$S_b = (\rho_u/\rho_b)S_u,$$

where S is the gas velocity relative to the flame front, ρ is the gas density, and the subscripts u, b refer to the unburned and burned gas respectively. Across a flame, unburned gas converts to higher temperature lower density burned gas. Consequently, the burned gas velocity relative to the flame must increase to maintain mass continuity. The resulting velocity field in the laboratory reference frame depends on the geometric constraints imposed by the combustion vessel.

Particle track visualization has been used to observe combustion generated flow in open bunsen flames for many years (Lewis and Von Elbe,

1943), and theoretical descriptions of such flows can be found in many combustion texts (Schelkin and Troshin, 1965, Strehlow, 1984). The study of combustion generated flows in confined geometries, however, is more complex because both the flame and the boundaries affect the flow. For example, combustion generated flow has been studied in fire research (Lee et al., 1983) and in I.C. engine combustion, both in the pre-chamber (Shimizu et al., 1983), and in the main chamber (Witze et al., 1984), but the complexity of these flows makes analysis difficult. The flow field associated with steady flame propagation in open channels is more tractable and has been studied both experimentally (Uberoi, 1959) and theoretically (Zeldovich et al., 1980). The flow field generated during flame propagation in closed tubes, however, has not been widely researched because the constant volume combustion process is nonsteady.

The present work is an experimental study of the fluid flow generated during nonsteady laminar premixed flame propagation in a constant volume combustion vessel. Early attempts to determine the flow field in closed volume combustion included the clever use of tracer flames (Ellis, 1928) and the use of aluminum strips hanging in the combustion vessel (Leyer and Manson, 1971). Recently, the combustion generated flow in closed tubes has been examined with laser Doppler anemometry (Dunn-Rankin et al., 1984, Starke and Roth, 1984) but determination of the flow field was incomplete in these studies. The present work extends the recent LDA studies by supplying a complete vector velocity map of the flow generated during combustion in a constant volume duct. A one-dimensional flame sheet model, Appendix I, is applied in the unburned gas to help analyze the experimental results.

APPARATUS

The experimental apparatus, Figure 1, consists of a constant volume combustion vessel, a pressure recording system, a laser Doppler anemometer (LDA), and a data acquisition microcomputer. The combustion vessel, constructed of 12.7 mm plexiglas, is 38 mm square by 155 mm. The plexiglas walls allow complete optical access to the combustion chamber. The flame starts from a single 3 mm spark gap located on the chamber axis approximately 10 mm from one endwall. Figure 2 shows the spark gap location, the direction convention adopted, and the coordinate layout of the combustion vessel. A pressure transducer (AVL 120P300), a charge amplifier (Kistler 5004E), an oscilloscope, and a polaroid oscilloscope camera record the chamber pressure during the combustion event.

The LDA operates in a standard forward scatter configuration. A 2 watt argon-ion laser, operated at 488 nm, provides the necessary coherent light. The laser power varies to optimize the LDA signal, but remains between 0.1 and 0.3 watt. The projection optics consist of a beam splitter of 50 mm fixed separation and a 295 mm focal length lens. Bragg cells differentially shift the resulting two beams to remove the directional ambiguity of the Doppler signal. The differential frequency is either 2 Mhz or 4 Mhz depending on the negative velocity expected. The projection optics rotate to measure either the radial (Y) or the axial (X) component of velocity. Aluminum oxide particles (approximately 1 micron), introduced into the inlet fuel/air flow by a spouted bed seeder, provide Doppler scattering sites. The collection optical system includes another 295 mm focal length lens, a secondary focusing lens, a plane mirror and a photomultiplier tube.

A TSI 1980A frequency counter analyzes the Doppler signal and outputs the validated velocity measurement to a microcomputer. The microcomputer (Compupro 6 Mhz Z80 microprocessor) samples and stores the time of the

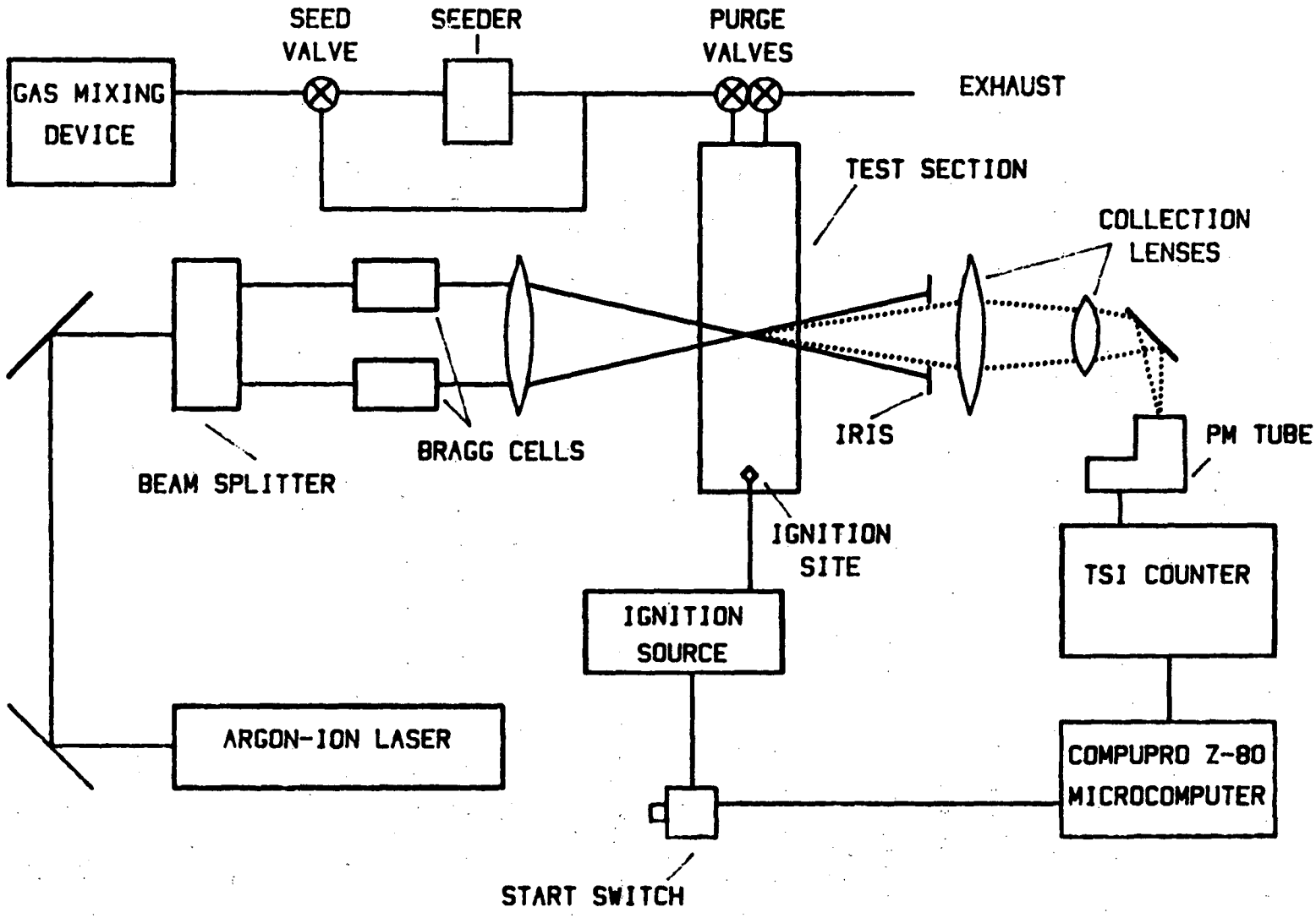

FIGURE 1. SCHEMATIC OF EXPERIMENTAL APPARATUS

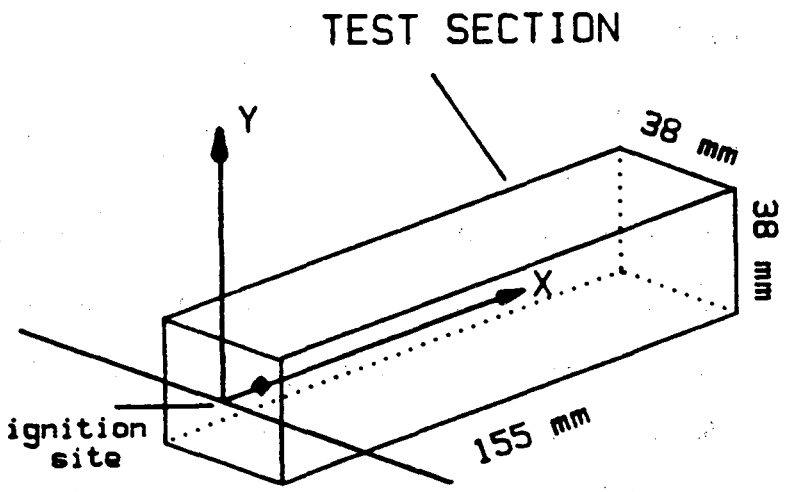

FIGURE 2. COORDINATE LAYOUT OF TEST SECTION

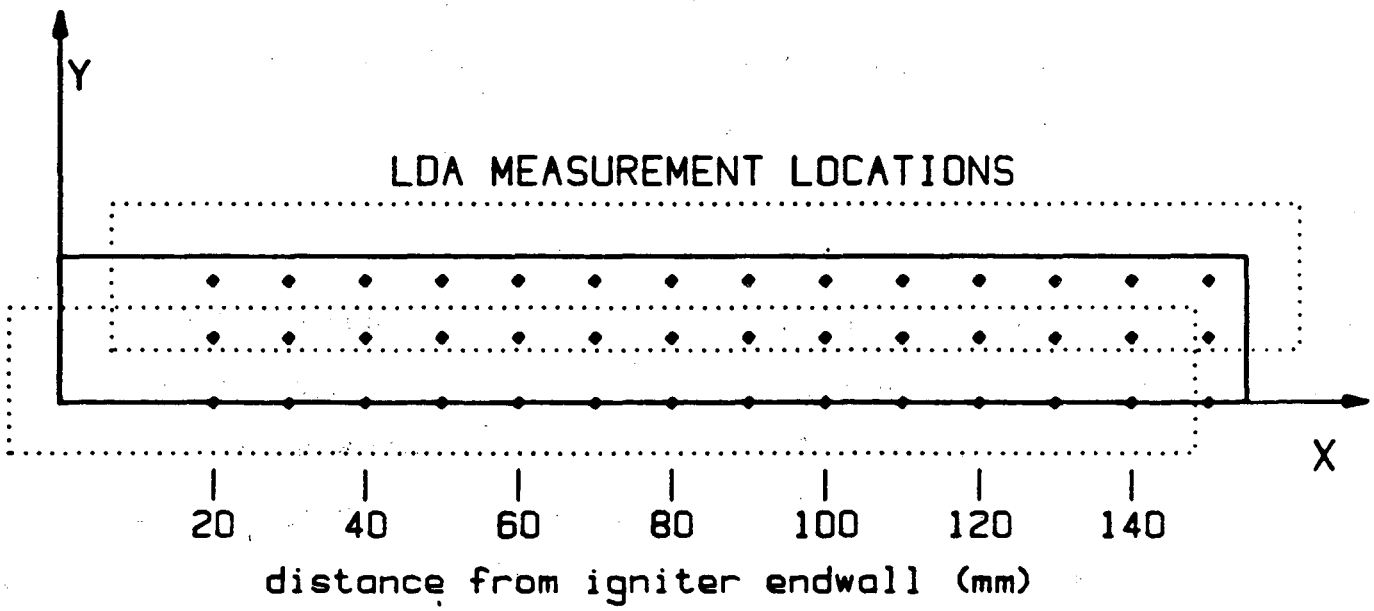

FIGURE 3. GRID OF LDA MEASUREMENT LOCATIONS

measurement and the value of the velocity at a minimum frequency of approximately 15 kHz.

METHODOLOGY

A stoichiometric mixture of methane/air purges the duct for a time sufficient for 20 complete changes of contents (approximately 45 seconds). The LDA seed is introduced into the inlet flow during the latter stages of the purging process. After purging, the gas motion within the combustion vessel settles (approximately 15 seconds). Ignition occurs when the LDA counter output is consistent with zero velocity.

Ignition simultaneously initiates combustion and triggers the data acquisition microcomputer. Each experiment records one component of velocity at a fixed location from t = 0 (the time of ignition) to t = 150 ms. Axial and radial components of velocity are measured at 42 locations inside the combustion vessel, Figure 3. The combination of these two components gives a velocity vector history at each measurement location. Five repeated measurements of each component at each location helps establish the run-to-run variations.

RESULTS

Figure 4a shows the raw axial velocity data at X = 100 mm and Y = 0 mm (the centerline). Five experiments are overlayed in the figure to indicate the run-to-run variability. The scatter of the data increases after the flame passes, but the variations are relatively small. Averaging the data in 0.5 ms windows and fitting the resulting average data with a smooth spline provides a curve representative of the velocity/time behavior at a single measurement point, Figure 4b.

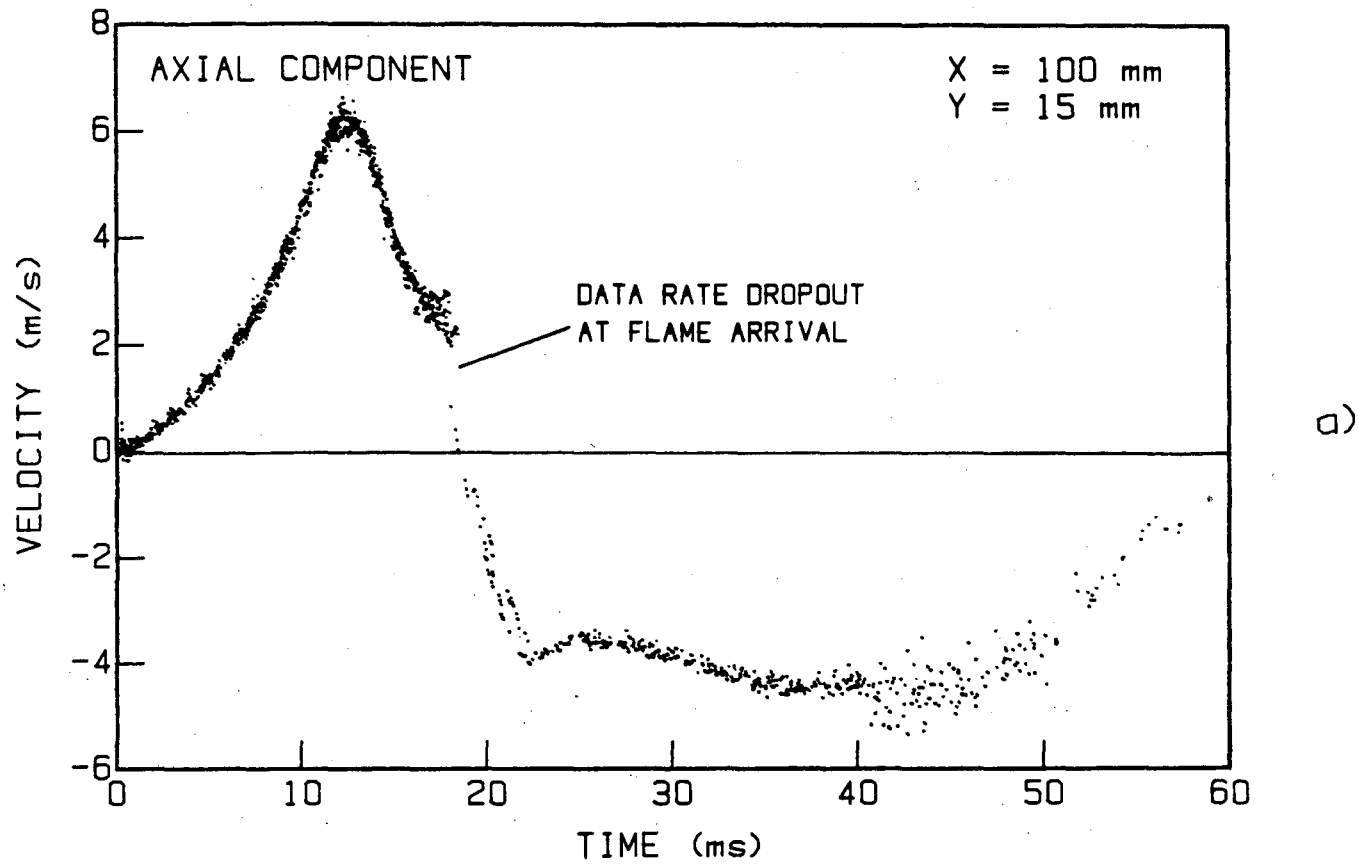

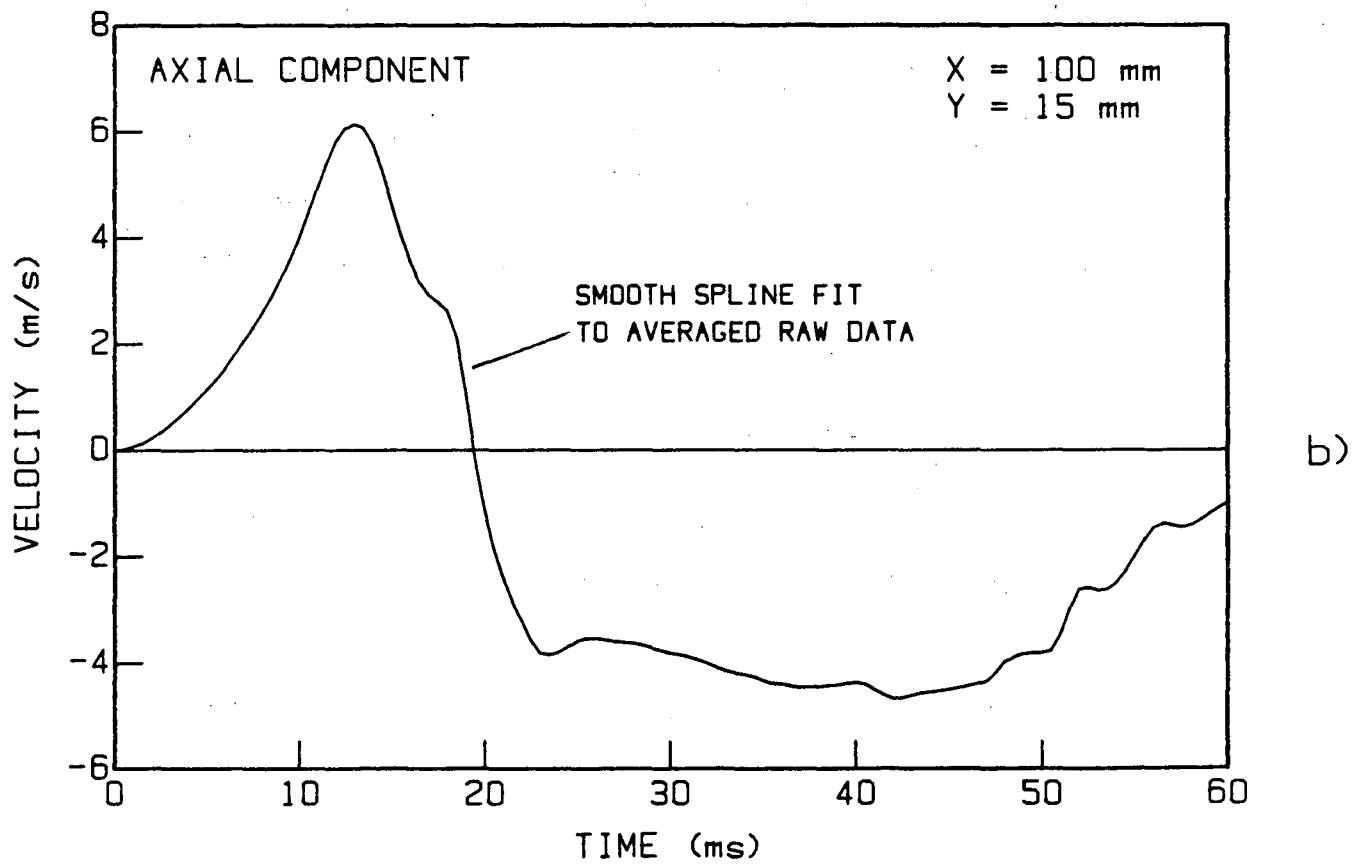

FIGURE 4. RAW DATA AND SMOOTH SPLINE FIT TO RAW DATA.
a) DATA RATE DROPOUT AT FLAME ARRIVAL
b) REPRESENTATIVE AXIAL VELOCITY

Flame Arrival

Noticeable LDA signal dropout accompanies the passage of the flame through the measurement volume, Figure 4a. The time of signal dropout represents the time of flame arrival at the LDA measurement point because the dropout is due primarily to decreased particle density in the expanded burned gas. The flame trajectories based on the time of LDA signal dropout are shown in Figures 5a (near the wall, Y = 15 mm), 5b (near the mid-radius, Y = 8 mm), and 5c (at the centerline, Y = 0 mm). Each data point represents the flame arrival time deduced from a single experiment. There are three sets of points and a kink in the flame trajectory at X = 95 mm because the flame actually reverses direction at this location. The reversal causes the LDA to measure in succession, unburned gas, burned gas as the flame passes, unburned gas a second time as the flame reverses, and finally burned gas again. The three sets of points represent the three flame passage times associated with this behavior. Figure 5d shows an approximate flame shape and position history computed from smooth splines fitted to the flame arrival data at each of the three radial positions. The approximate flame shape agrees well with high-speed schlieren cinematographic records of the flame propagation.

One-Dimensional Unburned Gas Flow

The velocity/time results indicate a nearly one-dimensional flow in the unburned gas except in the near vicinity of the flame front. The axial velocity/time traces for the three radial measurement locations (Y = 0, 8, 15 mm) at a single axial location are nearly identical until the flame arrives, Figure 6. This result agrees with the work of Starke and Roth (1984). The radial component of velocity at all measurement locations is approximately zero until the flame arrives, Figure 7. This observation further supports a one-dimensional assumption for the unburned gas motion.

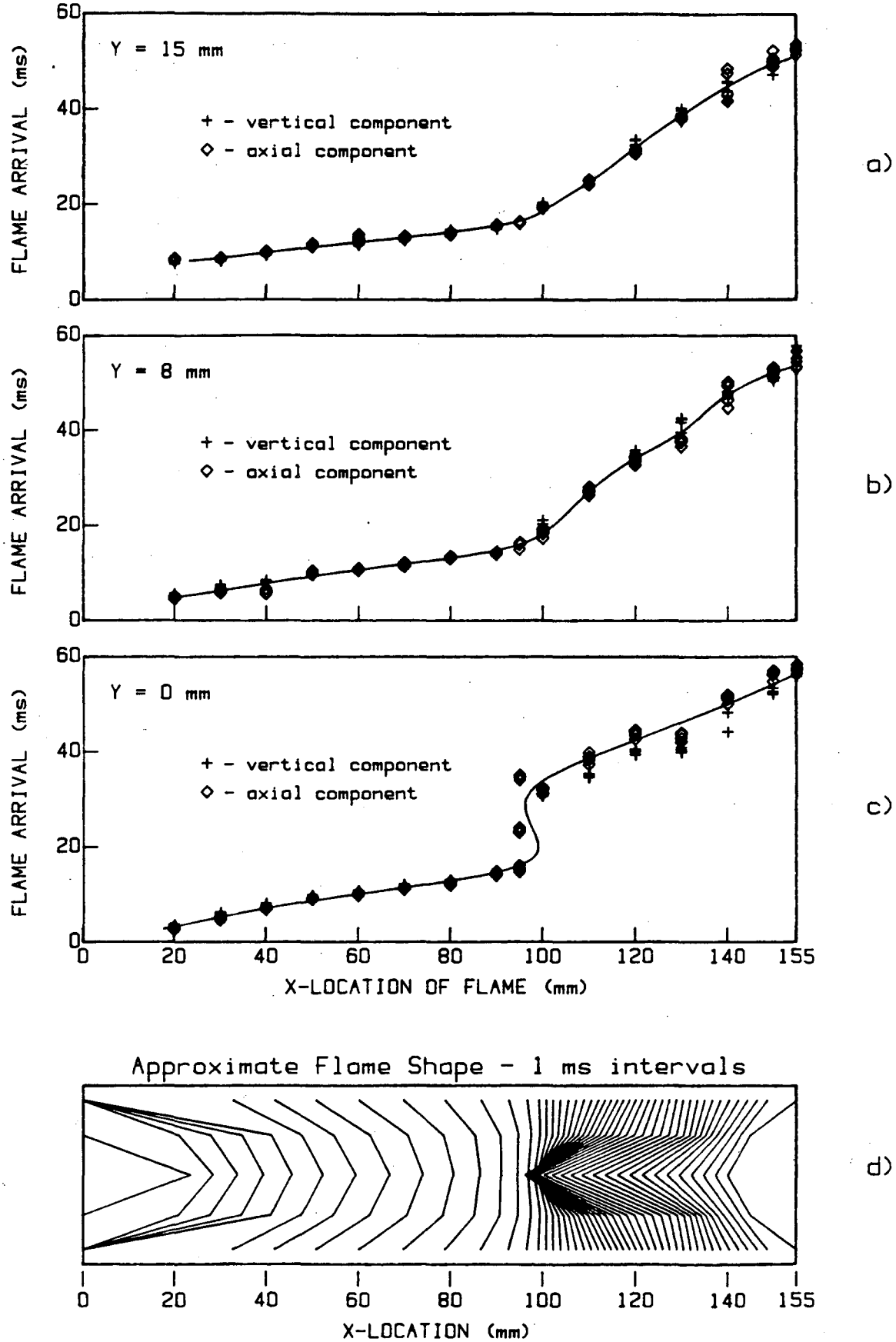

FIGURE 5. TIME OF FLAME ARRIVAL AT LDA MEASUREMENT LOCATIONS.
a) Y = 15 mm
b) Y = 8 mm
c) Y = 0 mm
d) FLAME SHAPE DEDUCED FROM FLAME ARRIVAL INFORMATION

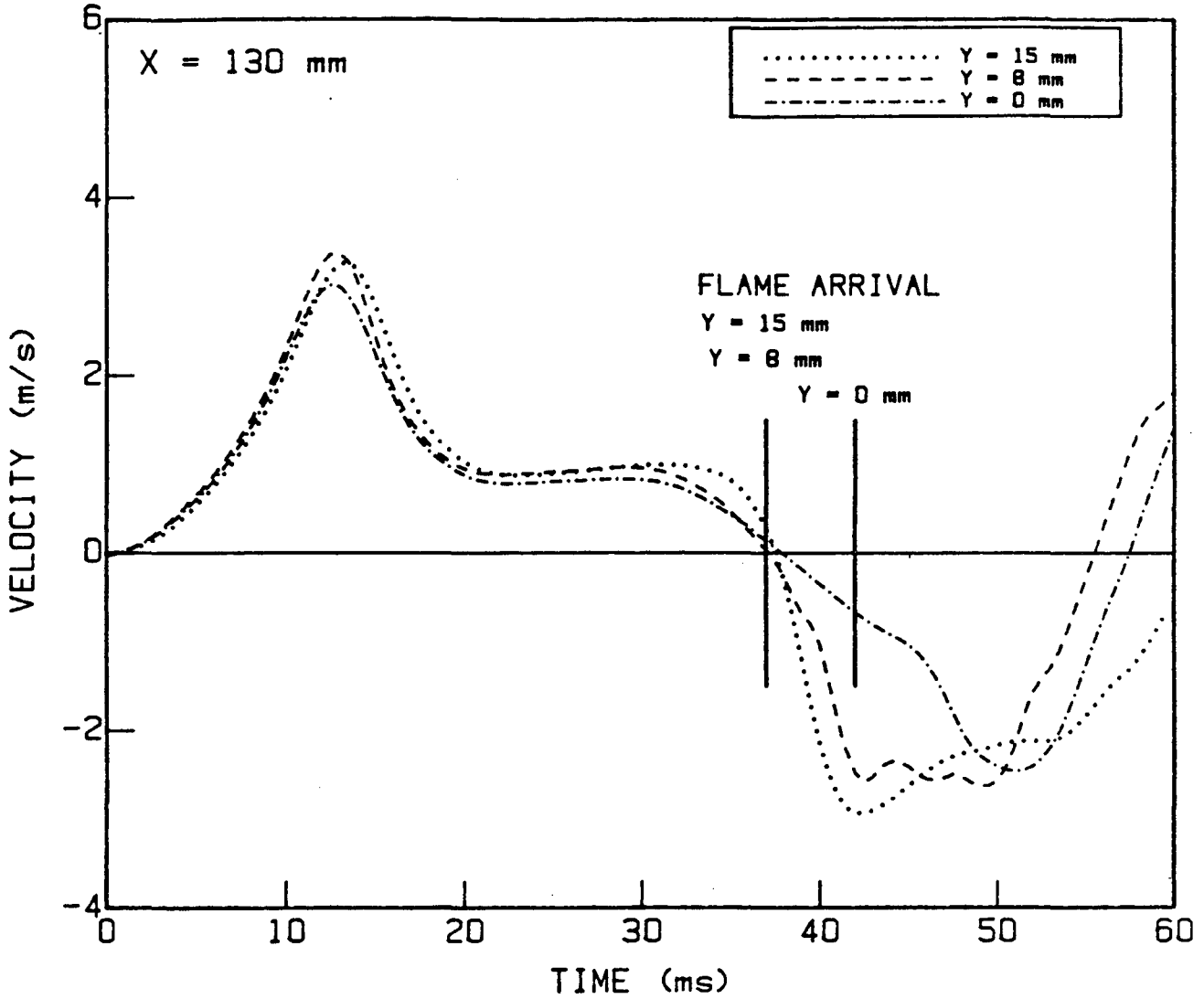

FIGURE 6. AXIAL COMPONENT OF VELOCITY AT X = 130mm FOR THREE RADIAL LOCATIONS.

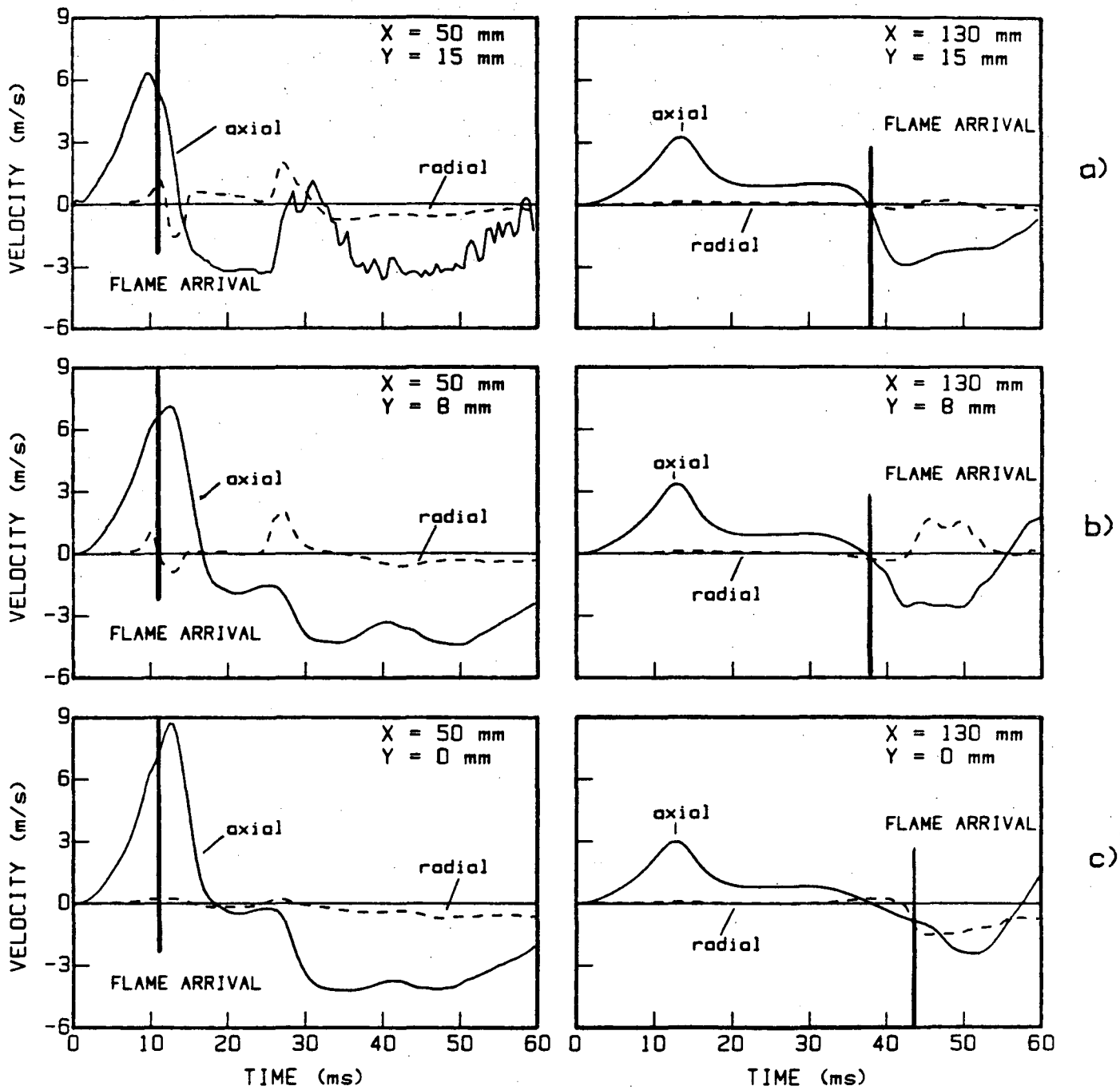

Figure 7. AXIAL AND RADIAL COMPONENTS OF VELOCITY SHOWING NEGLIGIBLE RADIAL VELOCITY BEFORE FLAME ARRIVAL.
a) Y = 15 mm
b) Y = 8 mm
c) Y = 0 mm

Velocity Vectors -- unburned gas

Figure 8 shows the velocity vector field during the flame propagation (vector scale: 1 mm = 2 m/s). The solid line indicates the flame location deduced from LDA signal dropout. The vector direction is away from the dot. The vectors below the centerline are mirrored from their counterparts above the centerline. The accuracy of this symmetry assumption was verified at several locations. High-speed schlieren movies of the flame propagation indicate that cylindrical symmetry, except in the corners of the duct, is likely.

The one-dimensional nature of the unburned gas flow described in the sub-section above is also evident in the vector field results. The only deviation occurs very near the flame front. The unburned gas velocity increases everywhere until approximately t = 12.5 ms. After this, the velocity decreases until approximately t = 20.0 ms and then it remains nearly constant. This surge behavior was noted also in an earlier study (Dunn-Rankin et al., 1984). The unburned gas velocity is highest at the flame front, and decreases to near zero at the endwall until t = 20 ms. After this time there is no obvious velocity maximum in the unburned gas. A flame cusp appears at approximately t = 17.5 ms, and the unburned gas has negative velocity within this cusp. The unburned gas outside the cusp has positive velocity throughout the combustion process.

Velocity Vectors -- burned gas

The burned gas velocity is positive until approximately t = 15 ms. Then, during a transition period (15 ms < t < 20 ms), the burned gas exhibits both positive and negative velocity regions. After t = 20 ms the burned gas velocity is entirely negative. Vortices appear in the burned gas just behind the flame near the side walls of the duct sometime between t =

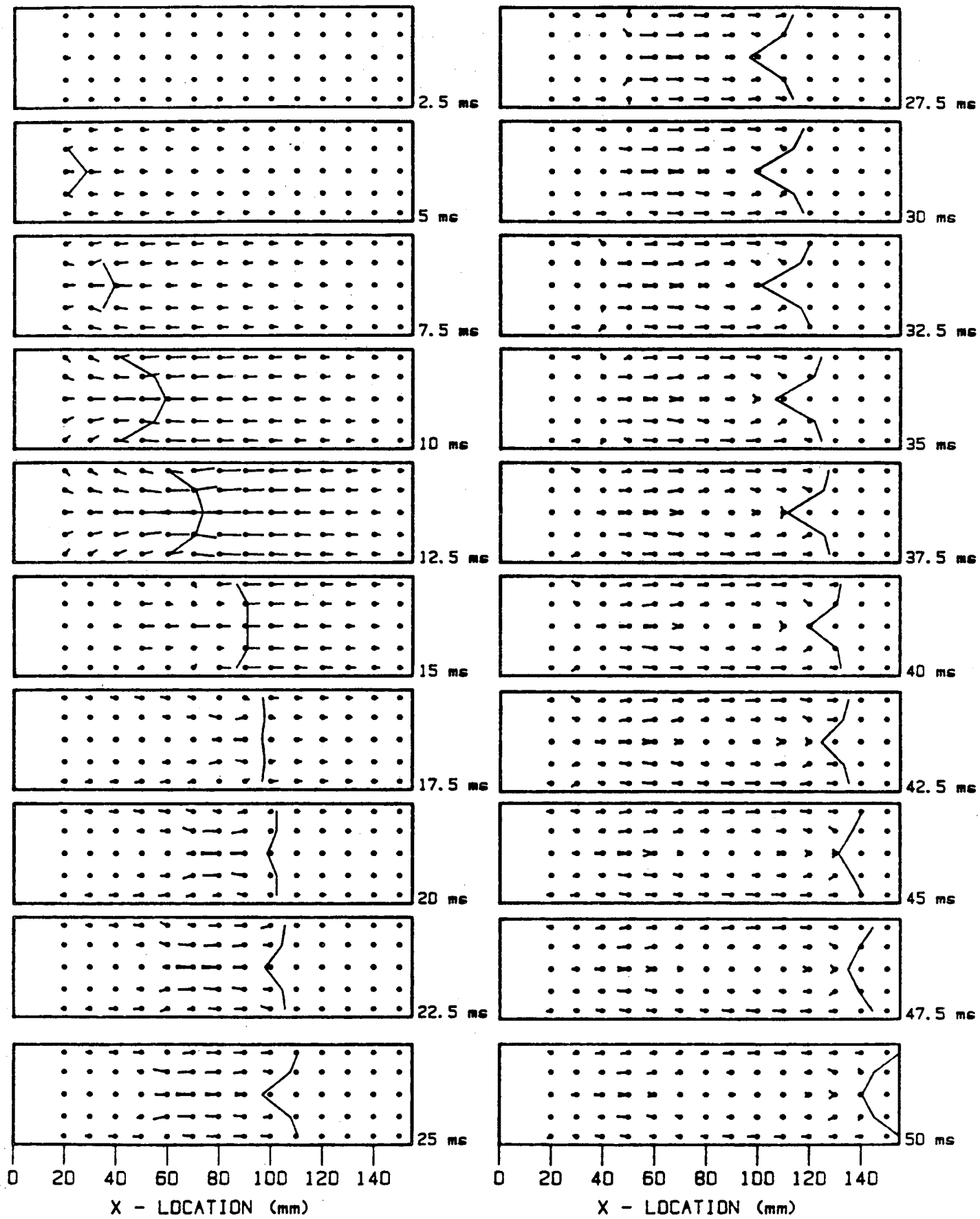

FIGURE 8. VECTOR VELOCITY HISTORY OF NON-STEADY FLAME PROPAGATION IN A CLOSED DUCT. SCALE: 1 mm = 2 m/s.

15 ms and t = 17.5 ms. Cylindrical symmetry makes the two individual vortices part of a single vortex ring. As the combustion proceeds, the vortex ring maintains its integrity and moves back through the burned gas, separating the burned gas into two regions. Between the vortex and the flame there is high velocity negative flow. Between the vortex and the ignition endwall there is low velocity negative flow. This behavior continues throughout the remainder of the flame propagation. The vortex is also visible in high-speed schlieren visualizations of the flame propagation.

Velocity Vectors -- near the flame cusp

The flow near the flame cusp has interesting features in both the unburned and the burned gas. The sides of the cusp drive the flow of unburned gas toward the duct centerline. This creates a stagnation point just within the flame cusp, resulting in negative velocity flow just within the flame cusp, while farther ahead of the flame the flow remains positive. The small negative velocity in the flame cusp was noted in an earlier study (Dunn-Rankin et al., 1984). In the burned gas, the cusp shaped flame creates a flow field similar to the flow expected around a solid body at the center of the duct. The burned gas flow deflects away from the centerline, and a stagnation region forms a short distance behind the point of the cusp. Flame generated stagnation regions have been discussed by Zeldovich (1981). Once the cusp ceases to grow (t > 35 ms), the burned gas flow field appears steady when viewed from the frame of reference of the flame.

A separate publication (Dunn-Rankin and Sawyer, 1985) discusses in detail the flame cusp and its relationship to the burned and unburned gas velocity field near the flame.

DISCUSSION

The burned gas behavior is complex because the flame shape influences the flow in the burned gas. The deflection of flow by a flame sheet (Maxworthy, 1961, Strehlow, 1984), and the generation of vorticity by a curved flame (Hayes, 1953) are examples of this influence. The character of the burned gas flow field changes during the flame propagation because both the flame shape and the magnitude of the unburned gas velocity are not steady. Once the flame shape and the unburned flow become steady (approximately t = 30 ms), the burned gas flow field also becomes steady (except for the remnants of the vortex generated earlier). The coupling of the burned gas fluid motion with the flame shape and the unburned gas flow makes quantitative discussion of the burned gas flow field difficult. The unburned gas flow field, however, except within the flame cusp, does not appear sensitive to the flame shape. Further, the measured one-dimensional nature of the unburned gas flow encourages the use of one-dimensional modeling to determine the major influences in the flow generation.

A one-dimensional model based on the unsteady continuity equation and the assumption of a linear increase in pressure with mass burned (Lewis and Von Elbe, 1964) is presented in Appendix 1. The predictions of the model are valid only for the unburned gas ($X > X_f$), and are summarized below:

1) The velocity decreases linearly from a maximum at the flame front to zero at the endwall:

$$V(X,t) = (1/\rho)(d\rho/dt)(L - X), \qquad (1)$$

where V is unburned gas velocity, ρ is the unburned gas density, assumed a function of time only, L is the chamber length, and X is the axial location.

2) The velocity magnitude can be related to the pressure and rate of pressure rise during the combustion. Equivalently the velocity magnitude can be related to the pressure and instantaneous flame area:

$$V = (1/\gamma P)(dP/dt)(L - X) \qquad (2)$$

or

$$V = S_u(1/\gamma)(1/(P_f-1))(P)^{(1/\gamma-1)}A_f(1-X^*), \qquad (3)$$

where P is the instantaneous pressure and P_f is the final pressure. The pressures are normalized by the initial pressure (1 atm). A_f is the flame area normalized by the cross-sectional area of the chamber, γ is the ratio of specific heats of the unburned mixture, X^* is the space variable normalized by the length of the chamber (L), S_u is the fundamental flame speed of the mixture.

Agreement between the experimental results and the linearity prediction (1) is very good, Figure 9. The figure shows the axial component of the centerline velocity in the unburned gas at several times during the combustion. Figures 6 and 7 show that the axial component of the centerline velocity is representative of the entire unburned gas flow. The velocity increases until approximately 12.5 ms, Figure 9a, and then decreases, Figure 9b. The velocity magnitude remains linearly decreasing with X throughout the velocity increase and decrease. The measured velocity does not go to zero at the endwall due to leaks out of the chamber end. The velocity at the endwall, obtained by extrapolation, provides an estimate of the leak loss from the chamber. The fraction of gas lost during the combustion is,

$$(m_l/m_o) = (\rho_{av}/\rho_o)V_{av}T_c/L \qquad (4)$$

where m_l is the mass loss through leaks, m_o is the initial mass in the combustion vessel, (ρ_{av}/ρ_o) is the ratio of the average leaking gas density to the initial gas density (approximately 2), L is the duct length (155 mm), V_{av} is the average extrapolated endwall velocity (approximately 0.4 m/s), and T_c is the total combustion time (approximately 50 ms). Equation (4) predicts that approximately 30 percent of the initial mass leaks out of the

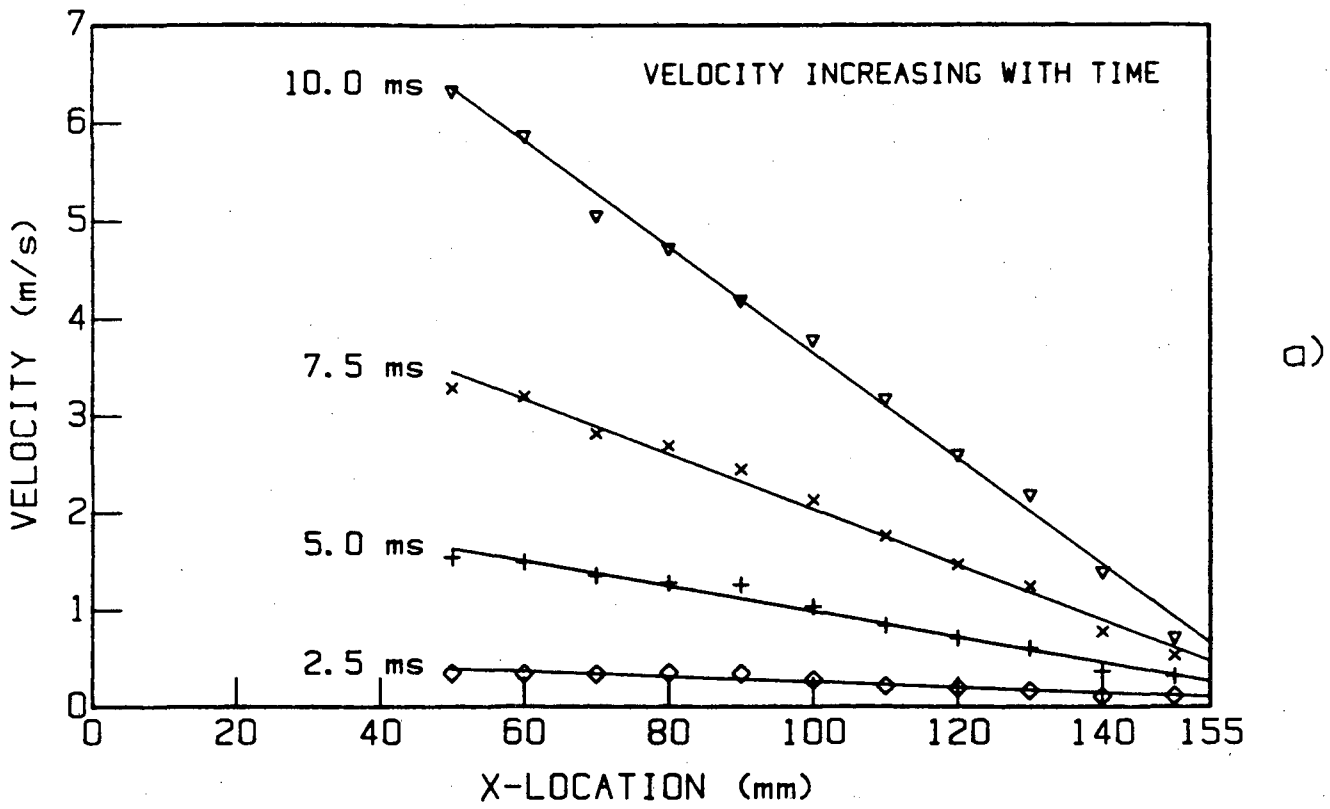

a)

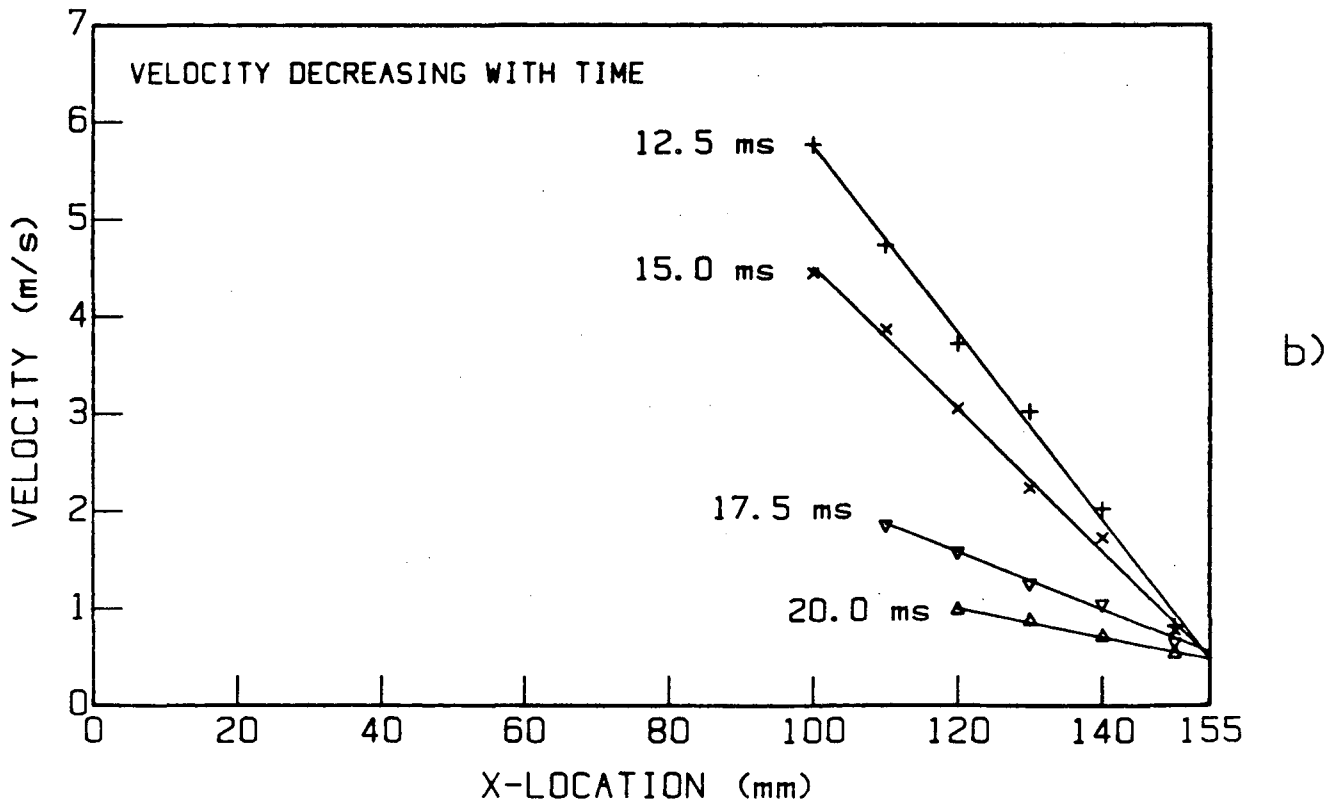

b)

Figure 9. AXIAL COMPONENT OF UNBURNED GAS VELOCITY SHOWING LINEAR DECREASE FROM THE FLAME TO THE ENDWALL.
a) t < 11ms
b) t > 11ms

vessel. Most of the leaking gas escapes through the open inlet and exhaust ports located in the endwall.

The recorded pressure during the combustion process, Figure 10, shows the effect of heat losses and leak losses from combustion vessel. At approximately t = 15 ms, the drop in pressure due to these losses is actually greater than the increase in pressure from the combustion process. It is difficult to separate the heat loss from the leak loss, but previous heat transfer work in a similar combustion vessel (Woodard et al., 1981), indicates that heat loss accounts for less than 20 percent of the difference between the measured pressure and the expected adiabatic pressure. Equation (2) uses the pressure information to predict the unburned gas velocity. Figure 11 compares the predicted velocity at X = 130 mm (dashed line) and the measured axial velocity (solid line) at the same location. Both curves have a velocity peak near t = 13 ms, but the measured velocity magnitude is much higher than the predicted velocity. The discrepancy arises from the inappropriate model assumptions of isentropic compression and zero velocity at the boundary. The magnitude of the leak from the combustion vessel gives a non-zero velocity at the endwall (X = L), and suggests an isothermal compression assumption for converting the density in equation (1) to the pressure in equation (2). With these new assumptions, equation (2) becomes,

$$V = (1/P)(dP/dt)(L - X) + V(L,t). \qquad (5)$$

Figure 11 also shows a comparison of the predicted velocity from equation (5) at X = 130 mm (dotted line) to the measured axial velocity at the same location (solid line). For simplicity, the prediction assumes that the endwall velocity, V(L,t), is linearly related to the pressure. The modified predicted velocity and the measured velocity are approximately equal until

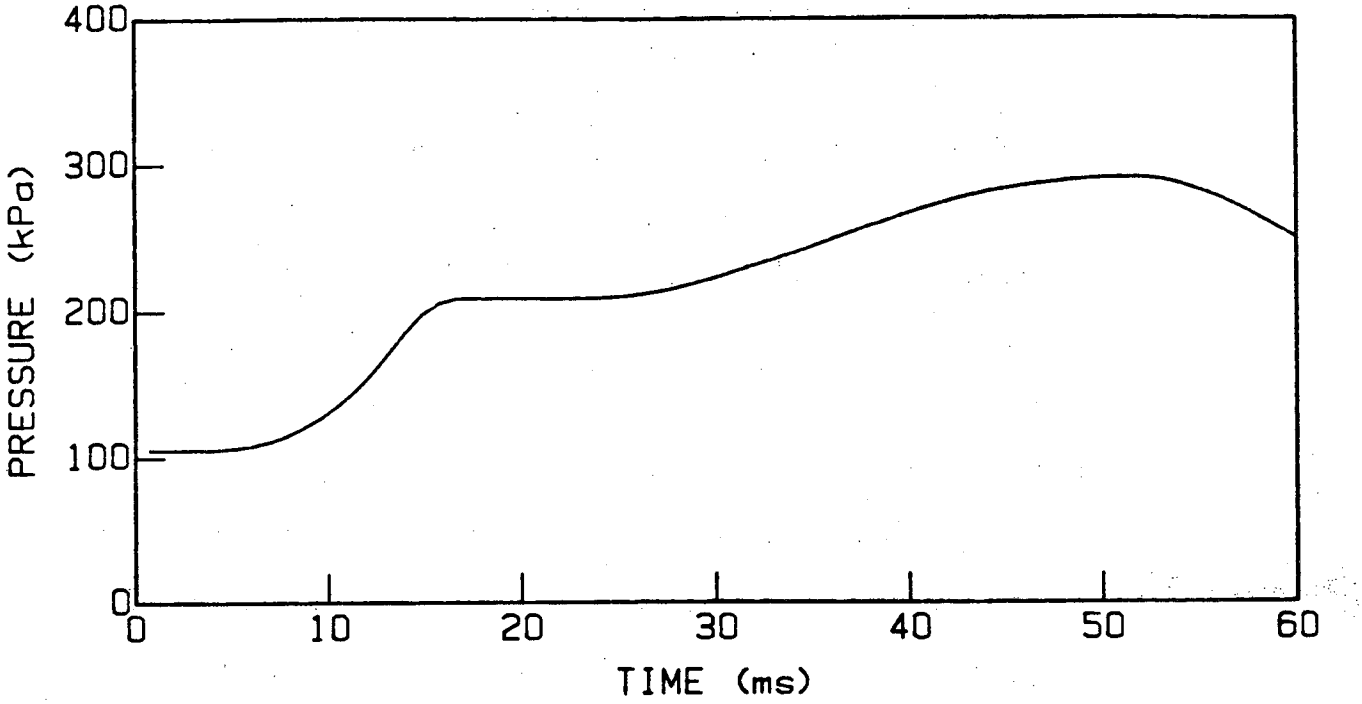

FIGURE 10. PRESSURE/TIME HISTORY OF COMBUSTION PROCESS.

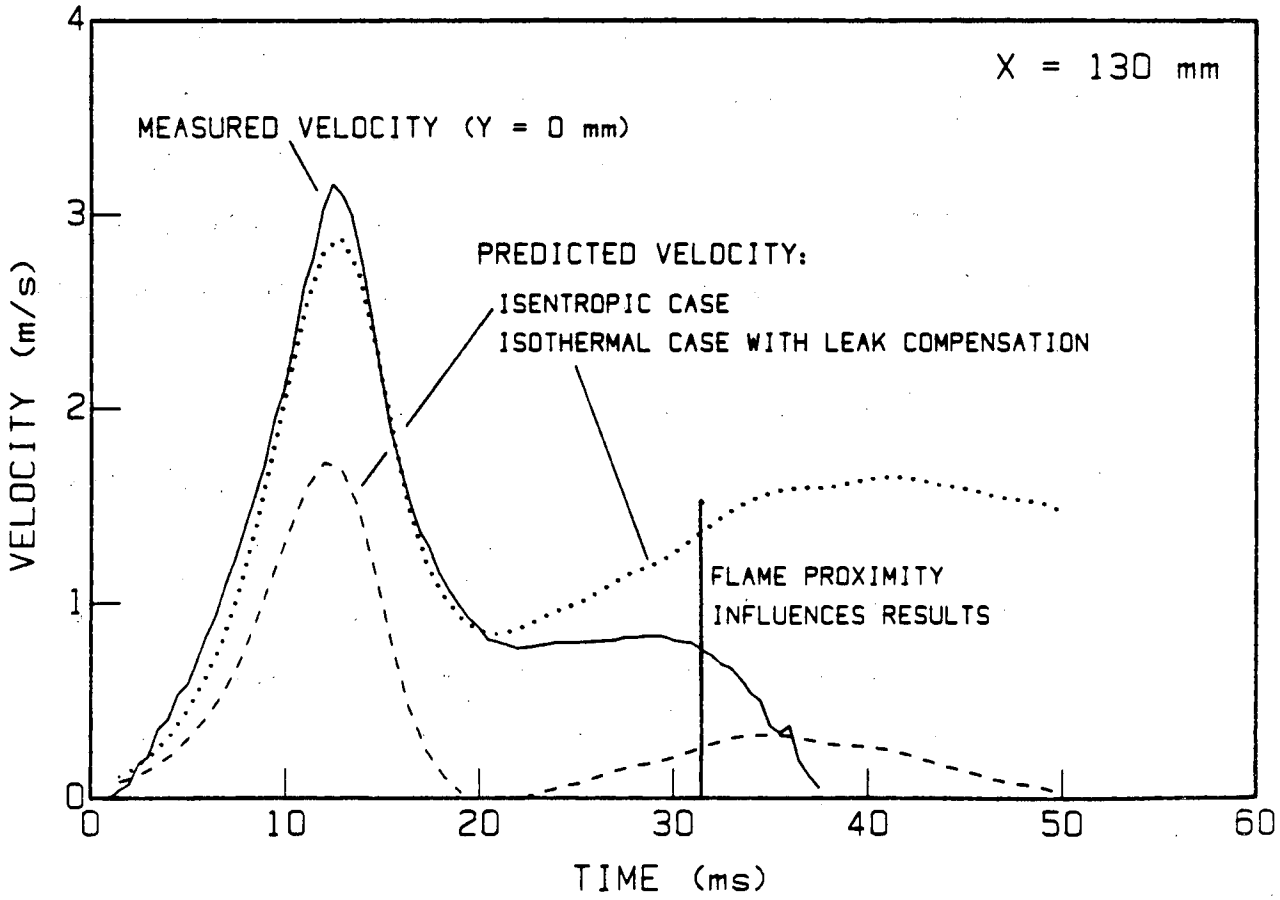

Figure 11. COMPARISON OF MEASURED AXIAL COMPONENT OF VELOCITY TO PREDICTED VALUE FROM ONE-DIMENSIONAL MODELS. X = 130 mm.

the flame influence begins to modify the measured velocity (approximately t = 35 ms).

All of the unburned gas velocity measurements show a velocity surge early in the combustion process (t < 20 ms), Figure 12. The equivalence of equations (2) and (3) indicates that the instantaneous flame area is the primary factor involved in the early velocity peak. The flame shape history, Figure 5d, shows that the maximum flame area coincides approximately with the maximum in the unburned gas velocity. Further, the decrease in unburned gas velocity following this maximum is accompanied by a rapid decrease in flame area. The precise flame area is difficult to determine because of the unknown complexities introduced by the corners of the duct and because the LDA dropout data does not provide information near the igniter or very near the walls. However, conversion of the approximate flame shape lines, Figure 5d, into surfaces of revolution about the duct axis, provides a rough estimate of the flame area variation with time. The approximate flame area/time curve, Figure 13, shows a definite peak early in the combustion. The peak occurs earlier than the measured velocity peak, because of the large inaccuracies in the flame area determination described above.

The accuracy of the one-dimensional model suggests that the expanding burned gas uniformly compresses the unburned gas. The area of the flame affects the rate of compression of the unburned gas, but the particular flame shape does not affect the predominantly one-dimensional nature of the unburned gas velocity field. The flame has a very short range influence on the unburned gas, but the compression from the combustion process affects the entire flow field.

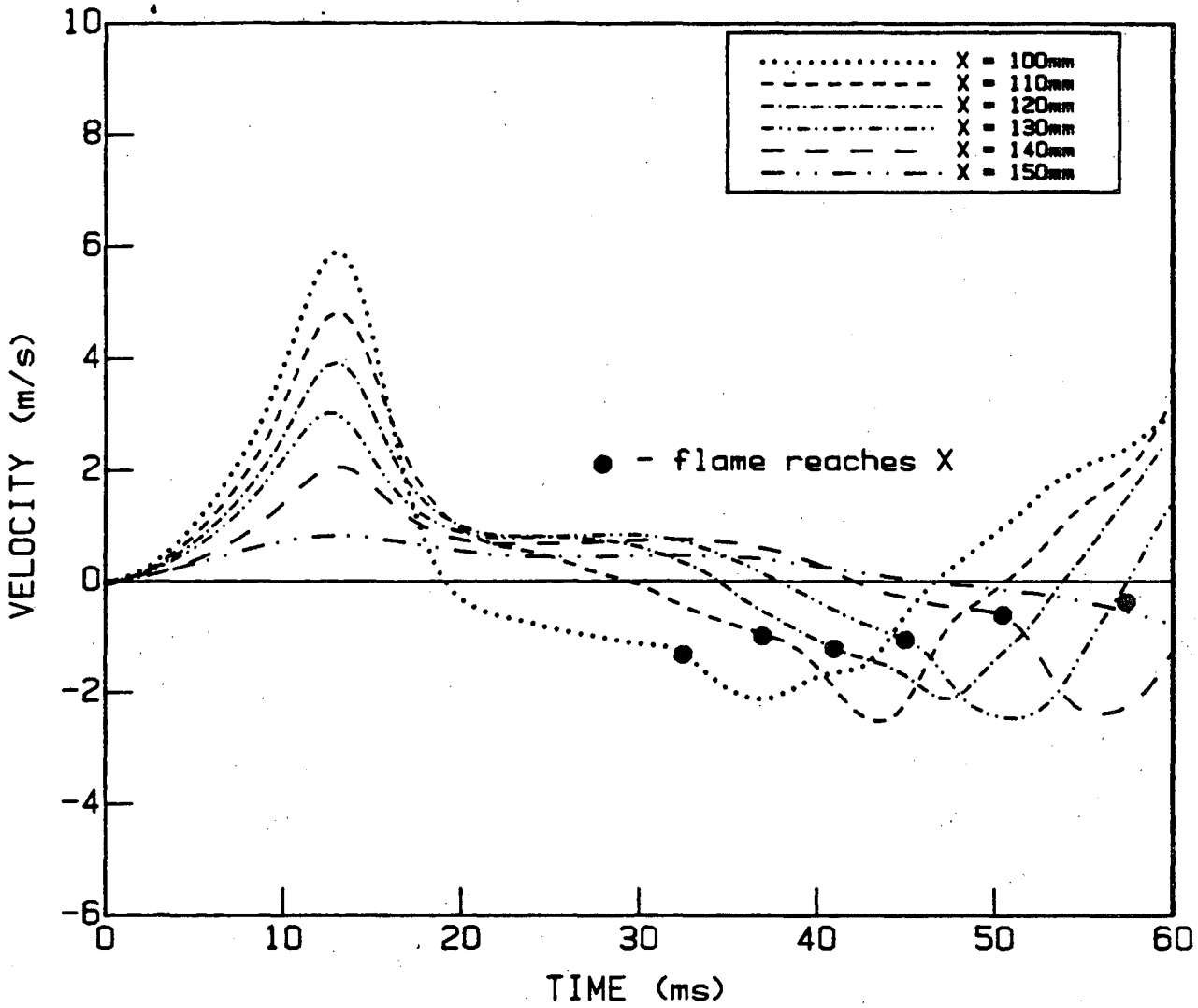

FIGURE 12. AXIAL COMPONENT OF VELOCITY AT VARIOUS MEASUREMENT LOCATIONS.

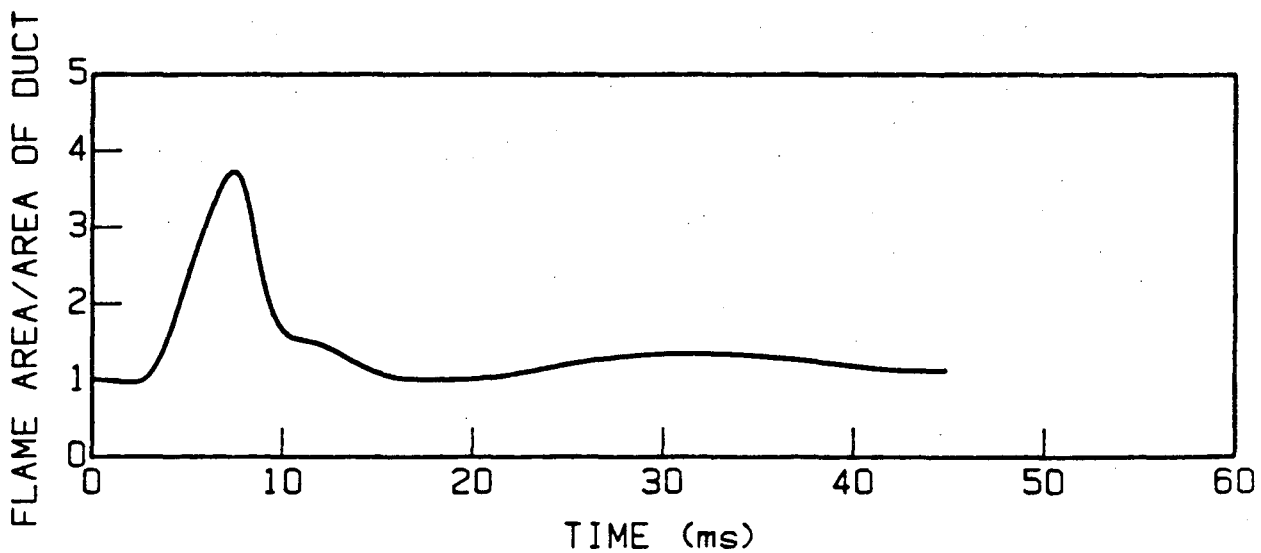

FIGURE 13. FLAME AREA DETERMINED FROM FLAME TRAJECTORY INFORMATION NORMALIZED BY THE CROSS-SECTIONAL AREA OF THE COMBUSTION VESSEL.

SUMMARY

This investigation uses laser Doppler anemometry to measure combustion generated flow during nonsteady premixed flame propagation in a closed duct. The measurements provide a complete vector velocity map of the unburned and burned gas motion during the combustion. LDA signal dropout, as the flame passes through the measurement volume, provides flame shape and position information.

The unburned gas velocity field is nearly one-dimensional for the entire combustion process. A simple one-dimensional model accurately predicts the unburned gas velocity behavior. The model suggests that the unburned gas, except very near the flame, undergoes a simple compression by the expanding burned gas. The rate of compression depends on the flame area, but the particular flame shape has no effect on the bulk unburned gas velocity field.

Both the flame shape and the unburned gas velocity magnitude influence the burned gas velocity field. During the early stages of combustion the burned gas velocity field is positive. Then, as the flame begins to form a cusp, a vortex ring forms in the burned gas just behind the flame front. In a few milliseconds, as the flame cusp grows, the burned gas velocity field becomes entirely negative. During the latter stages of combustion, a stagnation region appears within the negative burned gas velocity field a short distance behind the point of the cusp.

The results indicate strikingly different characteristics in the burned and unburned gas. The differences support two fluid (burned gas and unburned gas) approaches to fluid dynamic modeling in the presence of flames.

ACKNOWLEDGEMENTS

This work was supported by the Assistant Secretary for Conservation and Renewable Energy, Office of Transportation Programs, Division of Transportation Energy of the U.S. Department of Energy under contract number DE-AC03-76SF00098.

REFERENCES

Dunn-Rankin, D., Cheng, R.K., Sawyer, R.F. (1984). "LDA Study of Non-Steady Flame Propagation in a Constant Volume Duct." Presented at the Second International Symposium on Applications of Laser Doppler Anemometry to Fluid Mechanics. July 2-4, Lisbon, Portugal. Also Lawrence Berkeley Laboratory Report No. LBL-18150.

Dunn-Rankin, D., Sawyer, R.F. (1985). "The Interaction of a Laminar Flame with its Self-Generated Flow during Constant Volume Combustion." Submitted for presentation at the Tenth International Colloquium on Dynamics of Explosions and Reactive Systems.

Ellis, O.C. de C. (1928). "Flame Movement in Gaseous Explosive Mixtures (Part 7)." Fuel; a journal of fuel science, 7, 6, 502-508.

Hayes, W.D. (1957) "The Vorticity Jump Across a Gasdynamic Discontinuity." Journal of Fluid Mechanics, 2, 595-600.

Lee, J.H.S., Knystautas, R., Chan, C., Barr, P.K., Grcar, J.F., Ashurst, W.T. (1983). "Turbulent Flame Acceleration: Mechanisms and Computer Modeling." Presented at the International Meeting on Light-Water Reactor Severe Accident Evaluation, Cambridge, MA, August 28 - September 1. Sandia National Laboratory Report No. SAND83-8655.

Leyer, J.-C., Manson, N. (1971). "Development of Vibratory Flame Propagation in Short Closed Tubes and Vessels." Thirteenth Symposium (International) on Combustion, The Combustion Institute, Pittsburgh, Pennsylvania, 551-557.

Lewis, B., Von Elbe, G. (1943). "Stability and Structure of Burner Flames." Journal of Chemical Physics, 11, 75-97.

Lewis, B., Von Elbe, G. (1961). Combustion, Flames and Explosions of Gases. Academic Press, New York.

Maxworthy, T. (1961). "Discontinuity Properties of Laminar Flames." The Physics of Fluids, 4, 5, 558-564.

Shchelkin, K.I., Troshin, Ya.K. (1965). Gasdynamics of Combustion, Mono Book Corp., Baltimore.

Shimizu, S., Wakai, K., Sakai, S. (1983). "Combustion Processes and the State of Gases in a Divided Chamber." Proceedings of the 2nd International Pacific Conference on Automotive Engineering, Tokyo, Japan, November 7-10. Paper No. 830865.

Starke, R., Roth, P. (1984). "LDA Measurements in Cylindrical Vessel Explosions." Presented at the Second International Symposium on Applications of Laser Doppler Anemometry to Fluid Mechanics. July 2-4, Lisbon, Portugal.

Strehlow, R.A. (1984). Combustion Fundamentals. McGraw Hill Book Company, New York, New York.

Uberoi, M.S. (1959). "Flow Field of a Flame in a Channel." The Physics of Fluids, 2, 1, 72-78.

Witze, P.O., Martin, J.K., Borgnakke, C. (1984). "Fluid Motion During Flame Propagation in a Spark Ignition Engine." SAE Paper No. 840377.

Woodard, J.B., Hirvo, D.H., Greif, R., Sawyer, R.F. (1981). "Wall Heat Transfer and Flame Propagation in a Constant Volume Duct." Western States Section/The Combustion Institute Paper 81-51. Also Lawrence Berkeley Laboratory Report No. LBL-13021.

Zeldovich, Ya.B., Istratov, A.G., Kidin, N.I., Librovich, V.B. (1980). "Flame Propagation in Tubes: Hydrodynamics and Stability." Combustion Science and Technology, 24, 1-13.

Zeldovich, Ya.B. (1981). "Structure and Stability of Steady Laminar Flame at Moderately Large Reynolds Numbers." Combustion and Flame, 40, 225-234.

APPENDIX I -- ONE DIMENSIONAL MODEL FOR UNBURNED GAS

The unsteady continuity equation with a single space dimension is:

$$(1/\rho)(\partial\rho/\partial t) + dV/dX = 0, \qquad (1)$$

where ρ is the density, t is the time, V is the velocity, and X is the single space variable. Assuming ρ a function of time only, the continuity equation can be spatially integrated:

$$V(X,t) = (1/\rho)(d\rho/dt)X + g(t) \qquad (2)$$

Imposing the boundary condition of zero velocity at the endwall (X = L), the velocity field becomes linearly decreasing with X, but with a time varying magnitude controlled by the density:

$$V(X,t) = (1/\rho)(d\rho/dt)(L - X). \qquad (3)$$

The result (3) is only valid for the unburned gas ($X > X_{flame}$).

The pressure replaces the density by assuming isentropic compression of the unburned gas,

$$p = const(\rho^{\gamma}) \qquad (4)$$

and differentiating,

$$(1/\gamma p)(dp/dt) = (1/\rho)(d\rho/dt) \qquad (5)$$

hence,

$$V(X,t) = (1/\gamma p)(dp/dt)(L - X). \qquad (6)$$

With (6) the unburned gas velocity field can be determined from the pressure/time record of the closed volume combustion process alone.

The flame area can be related to the one-dimensional velocity in the following way:

Assuming a linear increase of pressure with mass burned (Lewis and Von Elbe, 1961),

$$m/m_o = (p - p_o)/(p_f - p_o) \qquad (7)$$

and differentiating,

$$(1/m_o)(dm/dt) = (1/(p_f - p_o))(dp/dt), \qquad (8)$$

where m is the mass burned; the subscript f refers to final conditions and subscript o refers to initial conditions. Another expression for mass burning rate comes from the definition of laminar flame speed, S_u,

$$dm/dt = \rho S_u a_f, \tag{9}$$

where a_f is the flame area. Replacing ρ with p from (4), the above equation becomes,

$$dm/dt = \rho_o(p/p_o)^{(1/\gamma)} S_u a_f. \tag{10}$$

Noting that $\rho_o = m_o/(a_c L)$, where a_c is the cross-sectional area of the chamber and L is the length of the chamber, and introducing $P = p/p_o$ and $A_f = a_f/a_c$, (10) becomes,

$$(1/m_o)(dm/dt) = (A_f S_u/L)(P)^{(1/\gamma)}. \tag{11}$$

Equating (11) and (8) and solving for dP/dt,

$$dP/dt = (P_f - 1)(S_u A_f/L)(P)^{(1/\gamma)}. \tag{12}$$

Replacing dp/dt in (6), an expression relating the velocity in the unburned gas to the flame area is,

$$V(X^*,t) = (1/\gamma)(P_f - 1)(P)^{((1/\gamma) - 1)}(A_f S_u)(1 - X^*), \tag{13}$$

where $X^* = X/L$. The velocity is linearly dependent on the flame area.

TECHNICAL INFORMATION DEPARTMENT
LAWRENCE BERKELEY LABORATORY
UNIVERSITY OF CALIFORNIA
BERKELEY, CALIFORNIA 94720